



# Diosgenin-loaded niosome as an effective phytochemical nanocarrier: physicochemical characterization, loading efficiency, and cytotoxicity assay

Mohammad Reza Hajizadeh<sup>1,2</sup> · Najmeh Parvaz<sup>1,2</sup> · Mahmood Barani<sup>3</sup> · Alireza Khoshdel<sup>1,2</sup> ·  
Mohammad Ali Fahmidehkar<sup>4</sup> · Mehdi Mahmoodi<sup>5</sup> · Masoud Torkzadeh-Mahani<sup>6</sup>

Received: 29 November 2018 / Accepted: 22 April 2019 / Published online: 27 May 2019  
© Springer Nature Switzerland AG 2019

## Abstract

**Background** The use of phytochemicals to prevent or suppress tumours is known as chemoprevention. Numerous plant-derived agents have been reported to have anticancer potentials. As one such anticancer phytochemical, diosgenin has several applications which are nevertheless limited due to its low solubility in water.

**Methods** We loaded diosgenin into niosome to increase its solubility and hence efficiency. Diosgenin-niosome (diosgenin loaded into niosome) was prepared by thin-film hydration method and characterised by optical microscopy, dynamic light scattering (DLS), scanning electron microscopy (SEM), and UV-visible spectrophotometry. Also, loading efficiency, in vitro drug release, and cytotoxicity assay were performed on HepG2 cell line.

**Results and discussion** Diosgenin-niosome has a nanometric size with a normal size distribution and spherical morphology. The loading efficiency of diosgenin was about 89% with a sustainable and controllable release rate. Finally, the viability of free diosgenin was 61.25%, and after loading into niosomes, it was improved to 28.32%.

**Conclusion** The results demonstrated that niosomes increase the solubility of naturally derived hydrophobic chemicals and thus enhance their anticancer effect.

**Keywords** Niosome · Diosgenin · Cancer · Release rate · Loading efficiency

## Background

Cancer is the most dangerous disease afflicting people around the world. Generally, the cause of most cancers is genetic mutations resulting from carcinogens such as tobacco smoke, radiation, and chemicals, and infectious agents promote these mutations [1]. Hepatic cancer is a fatal cancer [2], the fifth most common and third deadliest cancer worldwide [3] and the fourth cause of death from cancers in Asia and less developed countries [4]. Surgery, radiotherapy, chemotherapy, immunotherapy, and interventional therapy are common treatment methods for hepatic cancer [5]. Although treatment methods and chemotherapy drugs can inhibit the proliferation of liver cancer cells, their side-effects may be continued in the short and long term [6]. Because of numerous problems associated with chemotherapy, many patients prefer to use alternative medicines such as herbal therapies. Numerous studies have suggested that medicinal plants can be helpful for the treatment of cancers, specifically liver cancer [7].

✉ Masoud Torkzadeh-Mahani  
masoud.torkzadehmahani@gmail.com

<sup>1</sup> Department of Clinical Biochemistry, Faculty of Medicine, Rafsanjan University of Medical Sciences, Rafsanjan, Iran

<sup>2</sup> Molecular Medicine Research Center, Rafsanjan University of Medical Sciences, Rafsanjan, Iran

<sup>3</sup> Department of Chemistry, Shahid Bahonar University of Kerman, Kerman, Iran

<sup>4</sup> Research Center of Advanced Technologies in Medicine, Torbat Heydariyeh University of Medical Sciences, Torbat Heydariyeh, Iran

<sup>5</sup> Department of Clinical Biochemistry, Afzalipoor Faculty of Medicine, Kerman University of Medical Sciences, Kerman, Iran

<sup>6</sup> Department of Biotechnology, Institute of Science, High Technology and Environmental Sciences, Graduate University of Advanced Technology, Kerman, Iran

Due to the high bioavailability, limited side-effects, and low cost, plant extracts and their derivatives have been used for curing various diseases [8, 9]. Recent studies have demonstrated that some plant compounds such as steroidal saponins and sapogenins have anticancer effects [7, 10]. Diosgenin is a well-known steroidal sapogenin that can be useful for the treatment of various types of disorders [11]. This substance is abundantly found in several plant species such as *Costus speciosus*, *Smilax menispermoides*, species of *Paris*, *Aletris* and *Trillium*, species of *Dioscorea*, and *Trigonella foenum* [12]. Many studies have focused on the anticancer properties of diosgenin, and some authors mentioned that Diosgenin has antiproliferative activity in various tumoural cell lines, including prostate cancer [13], colon carcinoma [14], erythroleukemia (HEL cells) [15], squamous carcinoma [16], hepatocellular carcinoma [7, 17, 18], gastric cancer [19], lung cancer [20], and breast cancer [21–23]. Yan et al. (2009) evaluated the anticancer effect of diosgenin in the LA795 lung adenocarcinoma cell line using MTT assay [10]. Also, Selim et al. (2015) reported the anticancer effect of diosgenin on HepG2 cells [7]. Both reports confirmed that diosgenin has a considerable anticancer effect. The anticancer mechanism of diosgenin is thought to be the modulation of multiple cell signaling that plays a significant role in cell growth/proliferation, differentiation, migration, apoptosis, oncogenesis, and angiogenesis [24]. It has been suggested that the antitumor effects of diosgenin are mediated through induction apoptosis, activation of p53, cell cycle arrest, inhibition (STAT3& mtor) signaling pathway, and activation of caspase-3 [25].

Generally, diosgenin and other biologically plant-derived compounds have less toxicity than chemical drugs, but their free consumption can decrease their efficacy because of their low water solubility. Although numerous reports proved the anti-cancer potential of diosgenin, its pharmacological applications have been limited due to its poor water solubility (0.02 mg/L) [26], poor permeability, low bioavailability, and low stability in biological systems. Thus, a new and efficient method is required to enhance the solubility and anticancer effect of diosgenin [27–29].

Nanomedicine is one of the essential parts of nanotechnology with extensive applications in different areas, especially drug delivery [30–35]. Different nanocarriers are used for drug delivery, and niosomes are one of the best carriers [32, 36, 37]. Niosome is a vesicular nanoparticle composed of non-ionic surfactants and a helper lipid such as cholesterol that can increase the rigidity of the bilayer. Niosomes have high potential to target the tumour cell and show a controlled release in it. Niosomes are considered an alternative to other vehicles, specifically liposomes, due to their exciting properties such as simple preparation, low cost, high stability, and simultaneous encapsulation of hydrophobic and hydrophilic drugs [38]. Some authors mentioned that nanotechnology can enhance the application of diosgenin in medicine. Pathak et al.

(2018), for instance, employed chitosan/bovine serum albumin bilayers for improving the bioavailability of diosgenin. They found that the combination of biocompatible ionic polymers chitosan/BSA bilayer encapsulation around diosgenin allowed the sustained release of drug molecules up to 30 h [39]. Moreover, Wei et al. (2018) conjugated diosgenin derivatives to polyethylene glycol (PEG) with Schiff base bond as a pH-responsive drug delivery system to prevent thrombosis without increasing bleeding risk [40]. Despite the high efficiency of diosgenin loading in nanocarriers, there are a few reports on the loading of diosgenin in nanocarriers like niosomes for cancer therapy.

Due to the high demand of nano-phytochemicals, in this study, we loaded diosgenin into nano-niosome for enhanced solubility in biological systems and improved efficacy on HepG2 cell line. First, diosgenin was analysed by gas chromatography mass spectrometry (GC/MS), and then diosgenin-niosomes were prepared by thin-film hydration (THF) method. The size and morphology of the loaded formulations were characterised using dynamic light scattering (DLS), scanning electron microscopy (SEM), and light microscopy techniques. The loading efficiency and release rate of diosgenin from niosome were evaluated by dialysis bag and UV-visible spectroscopy. Finally, the anticancer effect of formulations was analysed by MTT assay on HepG2 cell line.

## Materials and methods

### Materials

Sorbitan monopalmitate (Span 40), dimethyl sulfoxide (DMSO), diosgenin ((3 $\beta$ ,25R)-spirost-5-en-3-ol, C<sub>27</sub>H<sub>42</sub>O<sub>3</sub>), and cholesterol ((3 $\beta$ )-cholest-5-en-3-ol) were obtained from Sigma (St. Louis, MO, USA). The human hepatocellular carcinoma (HepG2) cell line was purchased from the National Cell Bank of Pasteur Institute (Iran). RPMI-1640 was acquired from Gibco (USA). Polyoxyethylene sorbitan monopalmitate (Tween 40) was obtained from Quilmes Fine Chem Pvt. Ltd. (India). MTT reagent (1-(4,5-dimethylthiazol-2-yl)-3,5-diphenylformazan) was purchased from MELFORD Biolaboratories Ltd., UK. Finally, chloroform with analytical grade was purchased from Merck (Germany).

### Methods

#### GC/MS analysis

To identify the purity of diosgenin, a Varian CP 3800 gas chromatograph (Varian, Inc., Palo Alto, CA, USA) coupled with a Saturn 2000 MS/MS detector, a split-splitless injector, and an MS ChemStation were employed. The column was a

fused silica capillary CP-Sil 8 CB (5% phenyl groups in the dimethylpolysiloxane polymer, length of 30 m, ID of 0.25 mm, and film thickness of 0.25  $\mu\text{m}$ ) (Agilent J&W). The injector was set at 260 °C. the program of the oven started with 110 °C and increased to 200 °C at the rate of 3 °C/min. Helium was the carrier gas at the constant flow at 2 mL/min, and the sample (1  $\mu\text{L}$ ) was injected in the split mode (1:60). The data obtained from the sample were evaluated by the database of the instrument (NIST-MS).

### Preparation of formulations

Niosome formulations (blank niosome (niosome without diosgenin) and diosgenin-niosome (niosome with diosgenin)) were prepared by the THF method. The non-ionic surfactants (Span 40 and Tween 40), cholesterol, and diosgenin, dissolved in chloroform, at the molar ratio of 30:30:30:10, were added to a 50 mL round bottom flask. Afterward, chloroform was removed by a rotary evaporator (60 °C, 180 rpm) for 15 min (Heidolph, LABOROTA 4003-control-WB, Germany). The resulting lipid film was hydrated using 10 mL of phosphate buffered saline (PBS) (60 °C) for 30 min. For niosome purification, the obtained niosome formulations were centrifuged for 15 min at the speed of 15,000 rpm (MPW, MED INSTRUMENTS-150R, Germany). Finally, formulations were filtered with a 0.22 $\mu\text{m}$  membrane filter (Sartorius AG, Göttingen, Germany).

## Characterization of formulations

### Morphology

Formation of niosome and its morphology were evaluated by optical light microscopy. Optical micrographs were obtained by a camera (ICC50 W, Germany) attached to the optical

microscope (Leica DM500, Germany) at 10  $\times$  100 magnification at 25 °C. For a higher resolution, the size, shape, and topography of the formulations were also determined by SEM (SBC-12, KYKY, China) (2 kV). For this procedure, formulations were added to a double-sided carbon tape, positioned on an aluminium stub, and vacuum-dried. The samples were gold-coated by a Polaron E5100 for 3 min under an atmosphere of argon gas. The thickness of the Au coat was  $\sim$ 200 nm.

### Mean size and size distribution

The size distribution of niosome formulations was examined using DLS (Malvern Instruments). Briefly, 2 mL of samples was poured in a polystyrene cuvette and analysed at the diffraction angle of 90°.

### Loading efficiency

The amount of diosgenin entrapped into niosome formulations was spectrophotometrically determined using a UV-visible spectrophotometer (Agilent Technologies, Cary 60, USA) following a previously reported protocol [41, 42]. First, a calibration curve for diosgenin ethanolic solutions at different concentrations (1, 10, 50, 100, 200, 300, and 500 mg/L) was plotted. Total diosgenin content added to the niosome was 300 mg/L. After drug encapsulation, the loaded niosomes were dissolved in 1 mL of ethanol and then centrifuged at 15000 rpm for 20 min (model 5415D, Eppendorf, Germany). Free diosgenin absorbance in the supernatant was measured by the UV-visible spectrophotometer at the wavelength of 245 nm. Finally, the loading efficiency of the formulation was calculated as the difference between the total diosgenin amount added to niosome (300 mg/L) and the free diosgenin content measured in the supernatant by means of Eq. 1:

$$\text{Loading efficiency}\% = \frac{(\text{Total amount of diosgenin} - \text{Free diosgenin})}{\text{Total amount of diosgenin}} \times 100 \quad (1)$$

### Release rate of diosgenin from niosomes

The release assay was performed to understand the release behaviour of diosgenin encapsulated in niosome. Briefly, 1 mL of niosomes containing diosgenin was introduced into the dialysis bag, clipped from two ends, and placed in a beaker containing 30% (v/v) ethanol in 50 mL of PBS with pH 7.4 maintained at 37 °C with the help of a magnetic heater stirrer (Heidolph, MR3002G, Germany) (constant speed of 150 rpm) for 12 h. At specific time intervals, 1 mL of the released drug into PBS medium was withdrawn and immediately replaced

with 1 mL of fresh PBS buffer for sink condition. Withdrawn samples were analysed by a UV-visible spectrophotometer (Agilent Technologies, Cary 60 UV-visible, USA) at 245 nm. The percentage of the released diosgenin in PBS buffer was presented as % accumulative release. Data were reported in triplicate to confirm the reproducibility of results.

### Kinetic release study

The release kinetics of diosgenin from the niosome was assayed by means of different kinetic models such as zero-

order (Eq. 2), first-order (Eq. 3), Higuchi (Eq. 4), and Korsmeyer-Peppas (KP) models (Eq. 5) [43].

$$Q_t = Q_0 + k_0 t \quad (2)$$

$$Q_t = Q_0 e^{-k_1 t} \quad (3)$$

$$Q_t = k_H \cdot t^{1/2} \quad (4)$$

$$M_t/M = k_p t^n \quad (5)$$

where  $Q_t$  is the cumulative amount of released drug at time  $t$ ,  $M_t/M$  is the fraction of drug released, and  $k_0$ ,  $k_1$ ,  $k_H$ , and  $k_p$  are the constants for zero, first, Higuchi, and Peppas model, respectively. Also,  $Q_0$  is the total concentration of loaded drug and  $n$  is the diffusional exponent.

### Cell culture

The cells were cultured in RPMI-1640 (Gibco, USA) containing 10% FBS and 100 IU/ml penicillin-streptomycin under 5% CO<sub>2</sub> at 37 °C.

### MTT assay

HepG2 cell line was seeded in 96-well culture plates and allowed to adhere to the plate for 24 h in a humidified CO<sub>2</sub> incubator at 37 °C. Then, the culture medium was removed and cells were treated with diosgenin (10, 20, 30, 40, 50, 60, 70, 80, 100, and 150 μM) and diosgenin-niosome (40 μM) for 24 h. Next, 0.5 mg/mL of MTT was added to each well and incubated at 37 °C for 4 h in a dark place. Afterwards, MTT was removed, and 100 μL of DMSO was added to each well. Finally, absorbance was read at 570 nm using an ELISA plate reader (BIO-TEK INSTRUMENT, USA). The percentage of cell viability was determined using the following equation:

$$\text{Cell Viability (\%)} = \frac{\text{Abs T}}{\text{Abs C}} \times 100 \quad (6)$$

where Abs C is the absorbance of the control and Abs T is the absorbance of the test sample.

### Statistical analysis

One-way ANOVA was run for the statistical analysis of different experiments, followed by a posterior Bonferroni t-test. The  $p$  value <0.05 was considered significant. All values are reported as the mean ± standard deviation.

## Results and discussion

### GC/MS analysis of diosgenin

Alternative options is critically required to prevent the initiation and progression of human cancers. One of the exciting approaches is the use of medicinal plants or their isolated chemicals for the treatment of diseases, especially cancer. Diosgenin abundantly found in *C. speciosus* has several applications, especially in the pharmaceutical industry.

The GC/MS spectrum of diosgenin is presented in Fig. 1. As shown in the spectrum, there are two retention times, a small peak at 9.59 min corresponding to the solvent, and a significant peak at 27.5 min corresponding to diosgenin. Based on Fig. 1, despite the intense peak of diosgenin, there are some small peaks that were not counted due to their low intensity. It is evident from the spectrum that the purity of diosgenin is high, ~87%.

### Formulation characterization

Niosome vesicles were prepared using a conventional chloroform film method, generally used to prepare niosomes. A schematic representation of diosgenin-niosome before filtration procedure is illustrated in Fig. 2. Photomicrographs taken with a light microscope give the idea of shape attained by the vesicles. For this light, before the filtration procedure, optical microscopy was performed to evaluate the morphology of the prepared vesicles. Figure 3 depicts a micrograph image of formulations at the magnification of 100X. Spherical shapes with different sizes of niosomes were observed in the micrographs, but multi-layer vesicles (MLVs) were frequently observed. It can be seen that the external multilayered membrane is very clear, indicating that the niosomes have a bilayer and spherical structure. The loading of diosgenin into niosomes did not disrupt the structure and morphology of formulations. In formulations, no diosgenin or cholesterol crystal was observed. In a study conducted by Yeo et al. (2018), the formation and morphology of cinnarizine niosome was evaluated, and some round, circular shapes were observed under the light microscope, consistent with the images in our study [44].

The shape, size, and morphology of niosomes were observed by SEM (after niosome filtration). Figures 4 (a) and (b) show the SEM images of blank and diosgenin-niosome, respectively. SEM demonstrated nanometric niosomes with semi-spherical and closed vesicular structure without considerable aggregates. The diameter of niosomes was mainly in the range of 100–200 nm. After the loading of niosomes by diosgenin, the spherical integrity of formulations did not significantly change, but the size of diosgenin niosomes increased toward blank niosomes (100 nm for blank niosome increased to 170 nm for diosgenin niosome).

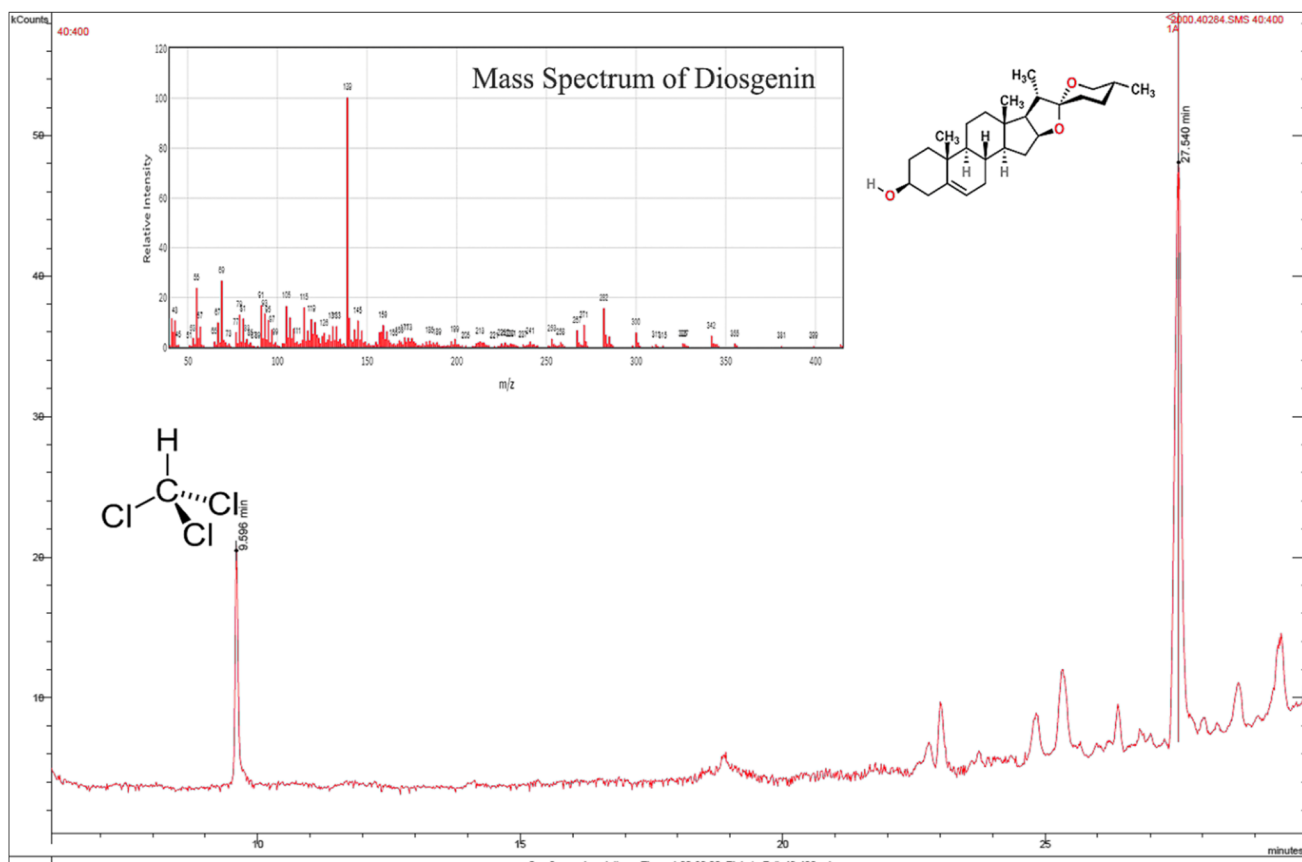


Fig. 1 GC/MS spectrum of diosgenin in chloroform

The size distribution of formulations measured by DLS is presented in Fig. 5. As shown in this figure, by loading diosgenin into niosomes, the size of vesicle did not significantly change ( $p > 0.05$ ). The particle size of blank niosome was  $99 \pm 2.5$  nm which increased to  $103 \pm 1.3$  nm for diosgenin niosome. The size distribution curves of both formulations had sharp patterns, indicating that niosomes have a standard size distribution. The homogeneity of the formulations was known as the polydispersity index (PDI). Small

values of PDI  $< 0.1$  indicate a homogeneous population, while a PDI  $> 0.3$  indicates high heterogeneity. The PDI value of blank niosome and diosgenin niosome was 0.21 and 0.22, respectively, revealing that both formulations have satisfactory homogeneity and stability.

Stability properties of formulations are dependent on the zeta potential. A zeta potential near  $\pm 30$  mV can guarantee a long-term stable formulation [45]. Zeta potentials for blank niosome and diosgenin niosome were  $-29$  mV and  $-36$  mV,

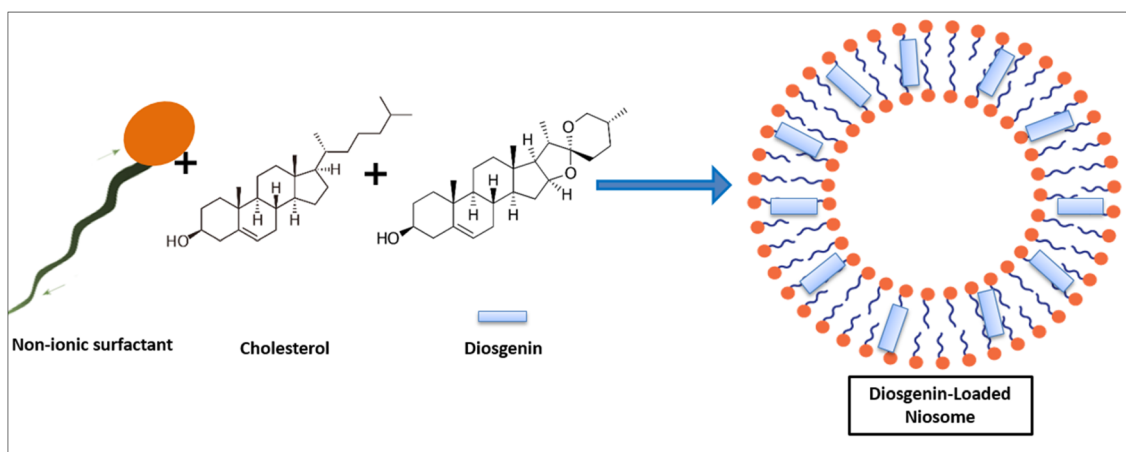
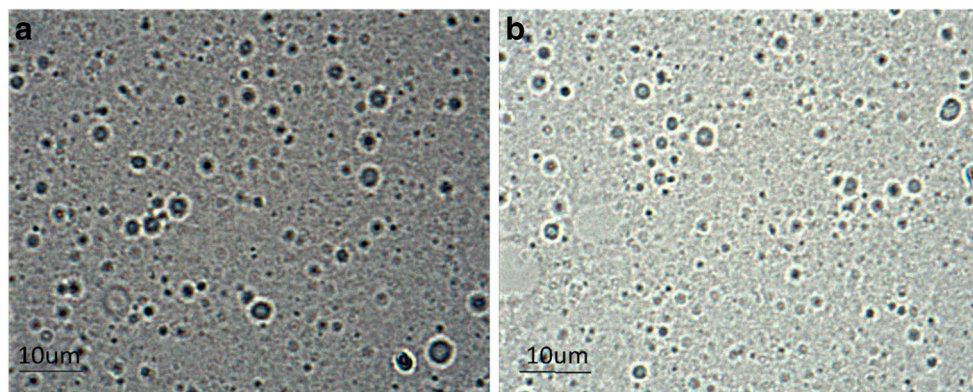


Fig. 2 Schematic representation of diosgenin niosome

**Fig. 3** Optical microscopic images of blank niosome (a) and diosgenin multilamellar niosome (b) before niosome filtration at the magnification of 100X



respectively (Fig. 6a and b). Loading of diosgenin into niosome resulted in more negative zeta values and hence more stable formulations.

Because of the hydrophobic nature of diosgenin, it will be loaded in the hydrophobic lipid shell of niosome. Loading of diosgenin into niosome is a physical absorption. Many studies mentioned that hydrophobic drugs are entrapped into the bilayer of niosomes through electrostatic interactions [38]. The loading efficiency of diosgenin in niosomes was relatively high and about 89%. Such high drug loading will be beneficial for the systemic administrations and results in the release of a significant amount of diosgenin at the site of action [46]. Barani et al. (2018) prepared Lawsone-loaded niosomes with

a particle size of 300 nm and loading efficiency of 69% [47]. The diosgenin niosome prepared in this study had a higher loading efficiency and smaller particle size in comparison to the one mentioned above. Also, Pando et al. [48] incorporated resveratrol into liposome and niosome to enhance its delivery to the skin. There were no important significant differences between the loading efficiency of niosomes and liposomes and the EE value (80%), showing that it has lower loading efficiency in comparison to the present study [48].

$$\text{Loading efficiency}\% = \frac{300 \frac{\text{mg}}{\text{L}} - 33 \frac{\text{mg}}{\text{L}}}{300 \text{ mg/L}} \times 100 = 89\% \quad (7)$$

**Fig. 4** SEM microphotograph of blank niosome (A and A') and diosgenin niosome (B and B')

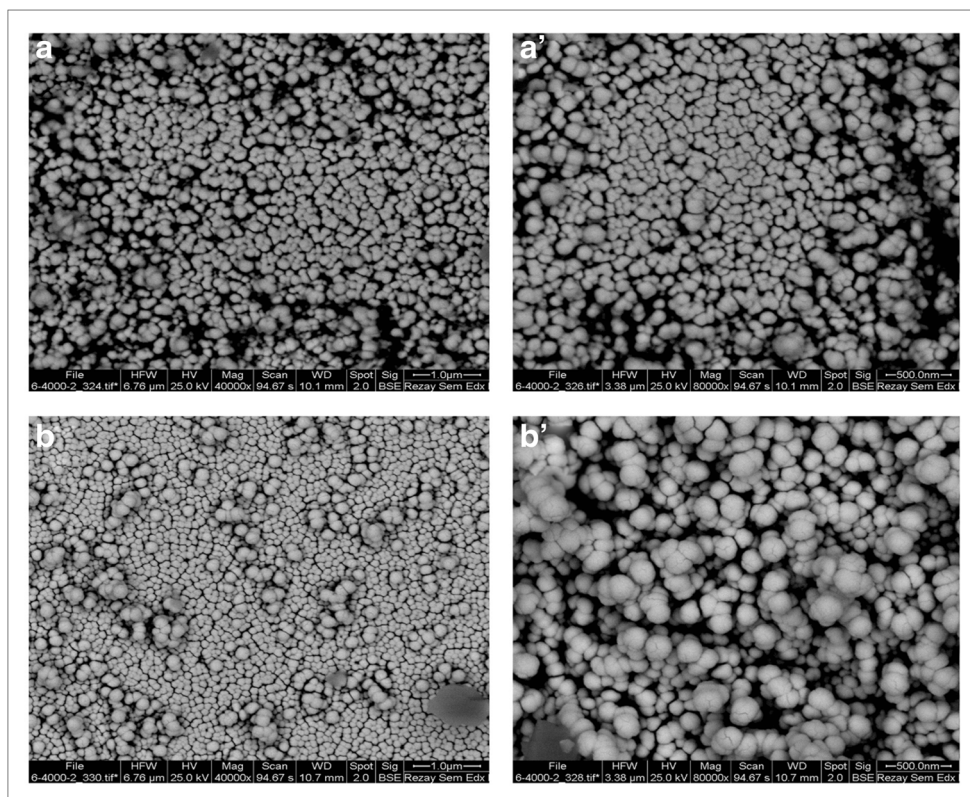
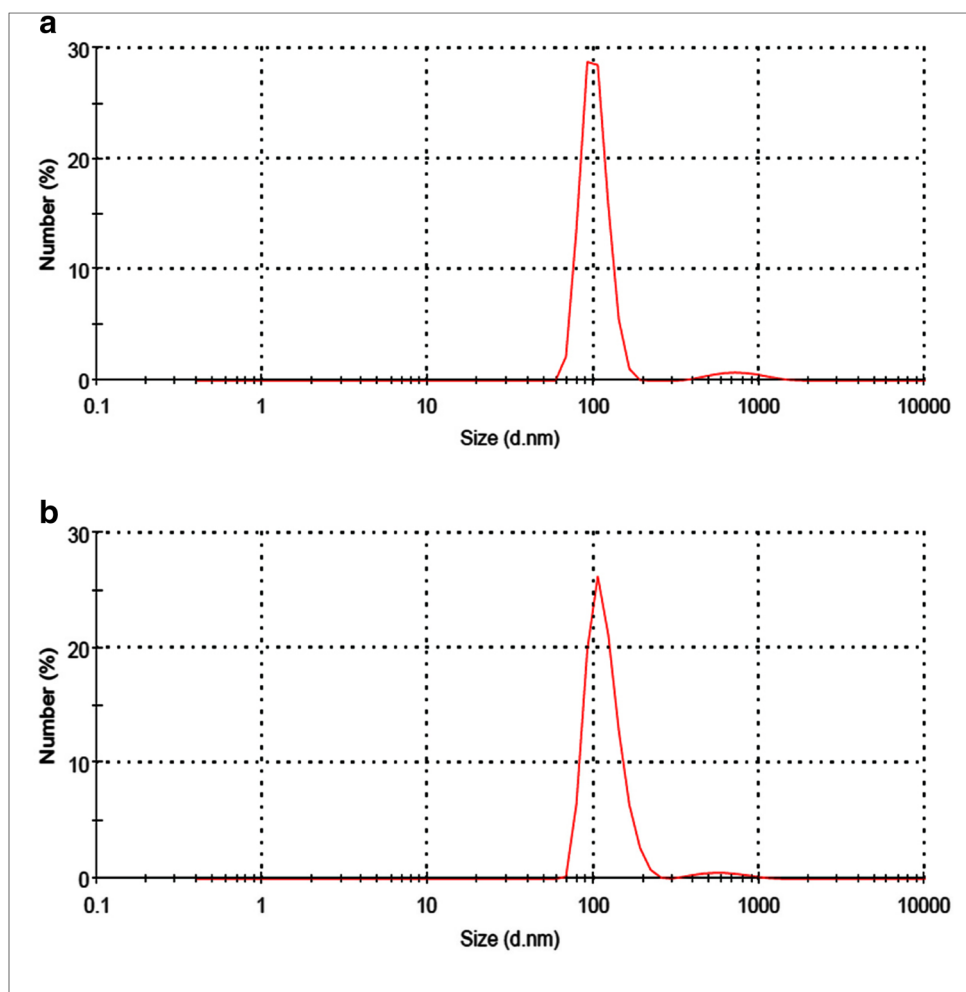


**Fig. 5** Particle size distributions of blank niosome (a) and diosgenin niosomes (b) based on DLS measurements



## Release study

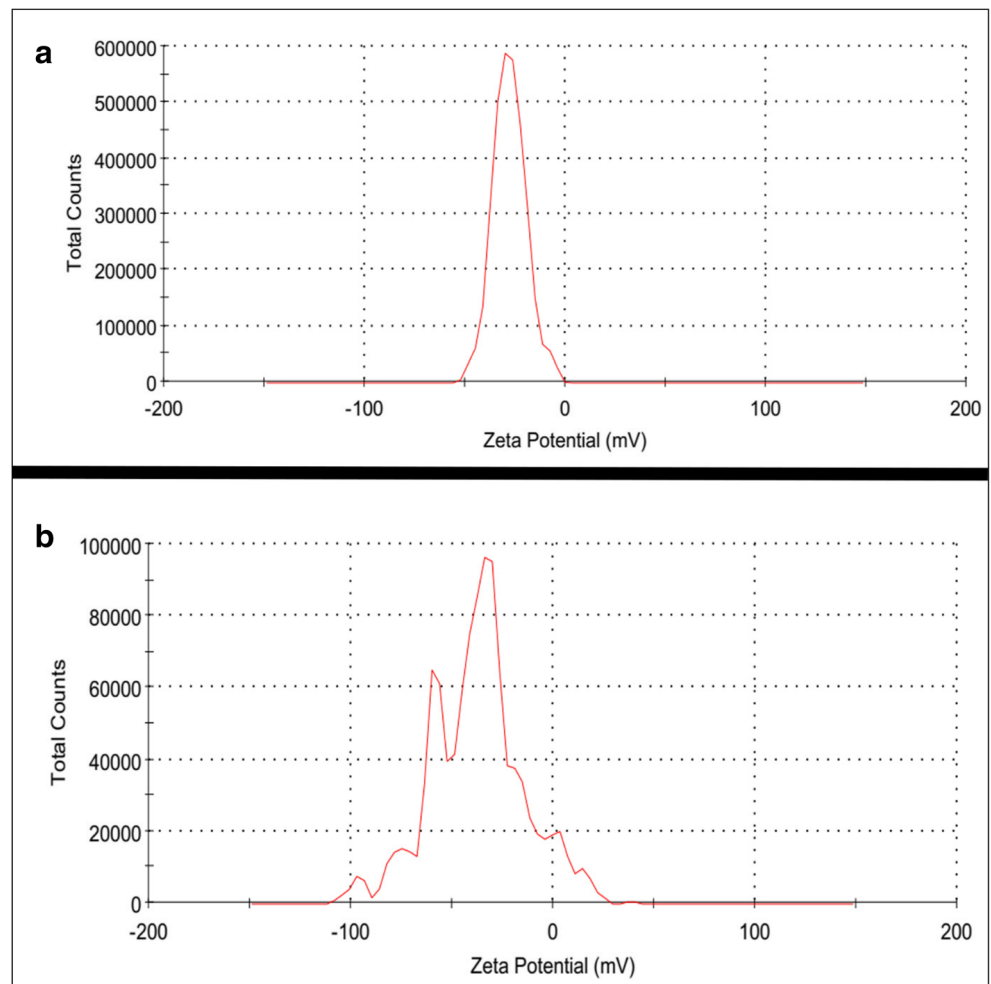
The release rate of drugs is an important parameter which has to be critically evaluated. In vitro studies are performed at physiological conditions (37 °C and pH 7.4) which can give an idea of in vivo performance. The in vitro drug release was performed here by the dialysis method. The samples were analysed in specific time intervals by a UV-visible spectrophotometer at 245 nm. The release profile is presented in Fig. 7. Interestingly, the cumulative percentage release of free diosgenin and diosgenin niosome significantly differed. For example, after 2 h, nearly all content of free diosgenin was released, while the diosgenin niosome showed a sustained release, such that after 12 h, only about 42% of formulations was released. Student t-test was run, showing a significant difference between the release rate of free diosgenin and diosgenin niosome ( $p < 0.05$ ). Because of the hydrophobic nature of diosgenin, it loaded in the bilayer part of niosome. Generally, hydrophobic drugs show a slow release rate

because of low diffusion. On the contrary, hydrophilic drugs demonstrate a faster release due to their high solubility in aqueous media. Different studies reported that the controllable and sustainable release of the loaded drug is a crucial factor for cancer therapy. Timmadonu et al. (2011) encapsulated hydrophobic paclitaxel into niosomes and evaluated its release rate [49]. Their formulation released ~81% of its loaded drug after 12 h. In another study, Jain et al. (2015) prepared duloxetine HCl-loaded nanoparticles for oral administration in which ~12% of the drug was released after 2 h [50]. Furthermore, Qi Xu et al. (2016) encapsulated curcumin in niosomes and concluded that curcumin release rate was ~55% after 12 h [51]. The above-mentioned studies reported that drugs loaded in niosomes show a sustainable release.

## Kinetic release study

The drug release kinetics was evaluated using zero-order, first-order, Higuchi, and KP kinetic models. Table 1 shows that the KP model best fitted the experimental data on the basis of the

**Fig. 6** Zeta potential of bank niosome (a) and diosgenin niosome (b) by DLS analysis



correlation coefficient ( $R^2 > 0.98$ ). This takes into account diosgenin diffusion and erosion controlled release processes from the niosome. Then, at the beginning in the presence of niosome might slightly expand and allow the Diosgenin within to diffuse through the interface.

### Cellular toxicity assay

Loading of hydrophobic drugs into niosomes can increase the toxicity of resulting formulations due to the enhanced solubility and improved interaction of niosomes and cancerous cells

**Fig. 7** In vitro release profiles of free diosgenin and diosgenin niosome in PBS 7.4 at 37 °C versus time (mean  $\pm$  SD,  $n = 3$ )

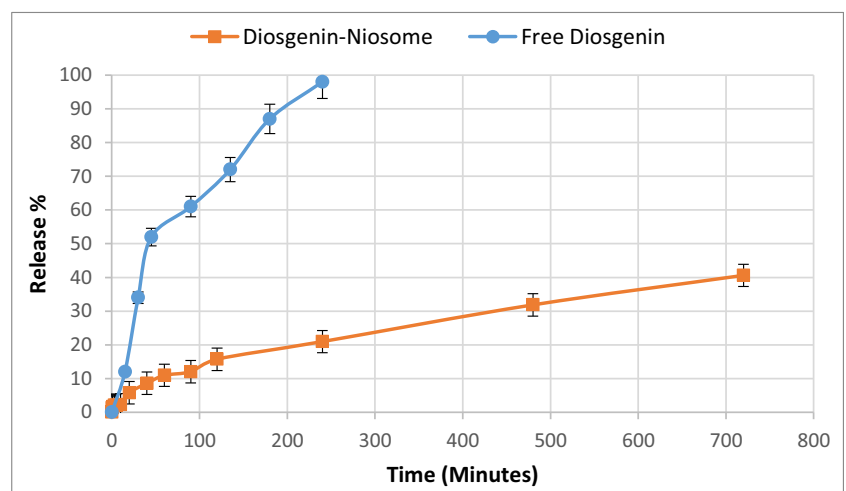




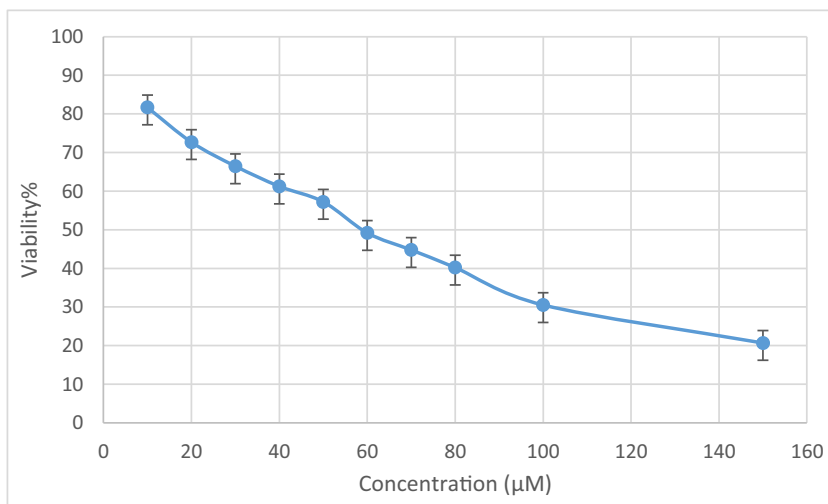
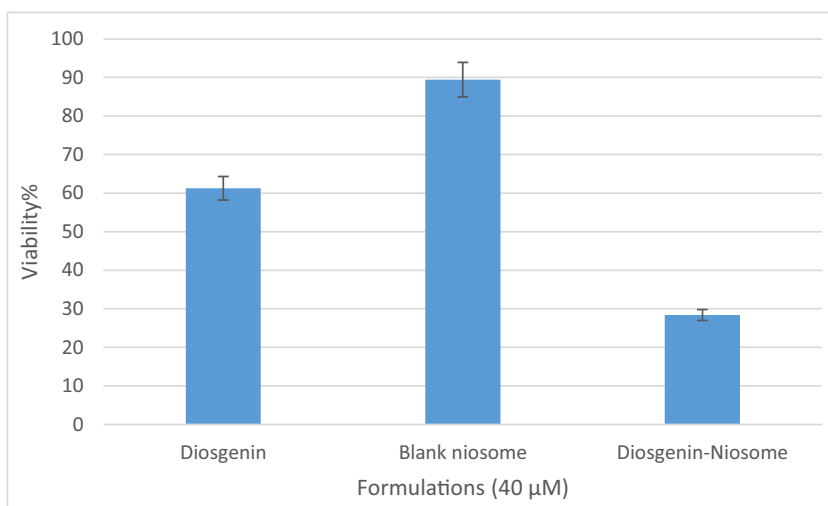
**Table 1** Models, equations, and regressions of diosgenin release from niosomes

Model	Equation	R <sup>2</sup>
Zero-order	$y = 0.1488x + 10.667$	R <sup>2</sup> = 0.9394
First-order	$y = 0.002x + 0.8998$	R <sup>2</sup> = 0.5464
Higuchi	$y = 0.5552x + 0.4285$	R <sup>2</sup> = 0.9223
KP	$y = 0.3016x + 0.0583$	R <sup>2</sup> = 0.9894

[47]. In order to verify this hypothesis, we studied the cytotoxicity of different concentrations of free diosgenin (10–150  $\mu\text{M}$ ) by MTT assay on HepG2 cancer cell line for 24 h (Fig. 8). Evidently, when the concentrations of diosgenin were increased, the toxicity of drug was increased.

Once again, when diosgenin was loaded into niosome, MTT assay was repeated. The *in vitro* cytotoxicity of free diosgenin, blank niosome, and diosgenin niosome was

evaluated on HepG2 cell line and presented in Fig. 9. For this comparison, we chose the concentration of 40  $\mu\text{M}$  of formulations. Blank niosome did not show significant cytotoxicity, and viability was  $\sim 89\%$ . The low toxicity of carrier guarantees the safety of its usage for healthy cells. Interestingly, cytotoxicity was significantly increased when diosgenin loaded into niosome. The viability of free diosgenin at the concentration of 40  $\mu\text{M}$  was 60%, and that of diosgenin niosome at the same concentration was 28% ( $p < 0.05$ ). Many authors mentioned similar results for phytochemical nano-delivery systems. For example, Hen et al. (2013) prepared cantharidin-entrapped niosomes, showing that the viability of cantharidin-niosome at the concentration of 40  $\mu\text{M}$  was lower than that of free cantharidin at the same concentration [52], consistent with our results. Moreover, Qi Xu et al. (2016) reported that curcumin-niosomes demonstrate enhanced cytotoxic activity against ovarian cancer cell line (A2780) in comparison to free curcumin [51], in line with our findings. These studies prove

**Fig. 8** MTT assay of free diosgenin in different concentrations (10–150  $\mu\text{M}$ ) (mean  $\pm$  SD,  $n = 3$ )**Fig. 9** The bar graph indicating the viability of formulations (40  $\mu\text{M}$ ) against HepG2 cancer cell lines after 24 h (mean  $\pm$  SD,  $n = 3$ )

that the loading of low-solubility phytochemical into niosome can improve their efficiency.

## Conclusion

Diosgenin as an efficient anticancer agent was loaded into niosomes, and its physicochemical characteristics were evaluated. The morphology of the resulting formulation was spherical with a standard size distribution. The loading efficiency of diosgenin was ~89%, and its release behaviour from niosome showed a sustained release compared to free diosgenin (40% in 720 min compared to 100% in 240 min). Finally, MTT assay proved that free diosgenin has no significant cytotoxicity (60% viability), whereas diosgenin niosome has a notable anticancer effect in HepG2 cancer cell line (28% viability). Therefore, this system can be employed as a promising carrier for a controllable, sustainable, and effective delivery for phytochemicals.

**Acknowledgments** The authors are grateful to the Graduate University of Advanced Technology, Kerman, Iran and Rafsanjan University of Medical Sciences, Rafsanjan, Iran for their excellent technical and financial support.

## Compliance with ethical standards

**Conflict of interest** There is no conflict of interest.

## References

- Radhi WA, Ismael SM, Al-Shawi JM, Hussein KA. Quantitative structure–activity relationship studies of flavonoids substituted as anticancer agents activity against the growth of the hepatic Cancer cell lines HepG2. *Int J Chem*. 2017;9(2):1.
- Wang W-W, Wang Y-B, Wang D-Q, Lin Z, Sun R-J. Integrin beta-8 (ITGB8) silencing reverses gefitinib resistance of human hepatic cancer HepG2/G cell line. *Int J Clin Exp Med*. 2015;8(2):3063–71.
- Chow EKH, Li F, Chen X, Bishop JM. Oncogene-specific formation of chemoresistant murine hepatic cancer stem cells. *Hepatology*. 2012;56(4):1331–41.
- Singh A, Dar MY, Joshi B, Sharma B, Shrivastava S, Shukla S. Phytofabrication of silver nanoparticles: novel drug to overcome hepatocellular ailments. *Toxicol Rep*. 2018;5:333–42.
- Yue M, Shen X, Liu Y, Lin X, Zhou S, Song Y. Effect of wilfortrine on human hepatic cancer HepG2 cell proliferation potential in vitro. *Genet Mol Res*. 2015;14(4):15349–55.
- Li WJ, Lian YW, Guan QS, Li N, Liang WJ, Liu WX, et al. Liver-targeted delivery of liposome-encapsulated curcuminol using galactosylated-stearate. *Exp Ther Med*. 2018;16(2):925–30.
- Selim S, Al Jaouni S. Anticancer and apoptotic effects on cell proliferation of diosgenin isolated from *Costus speciosus* (Koen.) Sm. *BMC Complement Altern Med*. 2015;15(1):301.
- Marrelli M, Cristaldi B, Menichini F, Conforti F. Inhibitory effects of wild dietary plants on lipid peroxidation and on the proliferation of human cancer cells. *Food Chem Toxicol*. 2015;86:16–24.
- Marzouk M, Soliman A, Omar T. Hypoglycemic and antioxidative effects of fenugreek and termis seeds powder in streptozotocin-diabetic rats. *Eur Rev Med Pharmacol Sci*. 2013;17(4):559–65.
- Yan L, Zhang Y, Gao W, Man S, Wang Y. In vitro and in vivo anticancer activity of steroid saponins of *Paris polyphylla* var. *yunnanensis*. *Experimental Oncology*. 2009;31(1):27–32.
- Janicka K, Jastrzebska I, Petelska AD. The equilibria of Diosgenin–phosphatidylcholine and Diosgenin–cholesterol in monolayers at the air/water Interface. *J Membr Biol*. 2016;249(4):585–90.
- Sethi G, Shanmugam MK, Warriar S, Merarchi M, Arfuso F, Kumar AP, et al. Pro-apoptotic and anti-Cancer properties of Diosgenin: a comprehensive and critical review. *Nutrients*. 2018;10(5):645.
- Chen P-S, Shih Y-W, Huang H-C, Cheng H-W. Diosgenin, a steroidal saponin, inhibits migration and invasion of human prostate cancer PC-3 cells by reducing matrix metalloproteinases expression. *PLoS One*. 2011;6(5):e20164.
- Lepage C, Léger D, Bertrand J, Martin F, Beneytout J, Liagre B. Diosgenin induces death receptor-5 through activation of p38 pathway and promotes TRAIL-induced apoptosis in colon cancer cells. *Cancer Lett*. 2011;301(2):193–202.
- Léger DY, Liagre B, Cardot PJP, Beneytout J-L, Battu S. Diosgenin dose-dependent apoptosis and differentiation induction in human erythroleukemia cell line and sedimentation field-flow fractionation monitoring. *Anal Biochem*. 2004;335(2):267–78.
- Das S, Dey KK, Dey G, Pal I, Majumder A, Maiti Choudhury S, et al. Antineoplastic and apoptotic potential of traditional medicines thymoquinone and diosgenin in squamous cell carcinoma. *PLoS One*. 2012;7(10):e46641.
- Kim DS, Jeon BK, Lee YE, Woo WH, Mun YJ. Diosgenin induces apoptosis in HepG2 cells through generation of reactive oxygen species and mitochondrial pathway. *Evid Based Complement Alternat Med*. 2012;2012:1–8.
- Li Y, Wang X, Cheng S, Du J, Deng Z, Zhang Y, et al. Diosgenin induces G2/M cell cycle arrest and apoptosis in human hepatocellular carcinoma cells. *Oncol Rep*. 2015;33(2):693–8.
- Mao Z-J, Tang Q-J, Zhang C-A, Qin Z-F, Pang B, Wei P-k et al. anti-proliferation and anti-invasion effects of diosgenin on gastric cancer BGC-823 cells with HIF-1 $\alpha$  shRNAs. *Int J Mol Sci*. 2012;13(5):6521–33.
- Mohammad RY, Somayyeh G, Gholamreza H, Majid M, Yousef R. Diosgenin inhibits hTERT gene expression in the A549 lung cancer cell line. *Asian Pac J Cancer Prev*. 2013;14(11):6945–8.
- Patel K, Gadewar M, Tahilyani V, Patel DK. A review on pharmacological and analytical aspects of diosgenin: a concise report. *Nat Prod Bioprospect*. 2012;2(2):46–52.
- Ghosh S, More P, Derle A, Kitture R, Kale T, Gorain M, et al. Diosgenin functionalized iron oxide nanoparticles as novel nanomaterial against breast cancer. *J Nanosci Nanotechnol*. 2015;15(12):9464–72.
- Sung B, Prasad S, Yadav VR, Aggarwal BB. Cancer cell signaling pathways targeted by spice-derived nutraceuticals. *Nutr Cancer*. 2012;64(2):173–97.
- Raju J, Rao CV. Diosgenin, a steroid saponin constituent of yams and fenugreek: emerging evidence for applications in medicine. In: *Bioactive compounds in Phytomedicine: InTech*; 2012.
- Jesus M, Martins AP, Gallardo E, Silvestre S. Diosgenin: recent highlights on pharmacology and analytical methodology. *J Anal Methods Chem*. 2016;2016:1–16.
- Binesh A, Devaraj SN, Halagowder D. Atherogenic diet induced lipid accumulation induced NF $\kappa$ B level in heart, liver and brain of Wistar rat and diosgenin as an anti-inflammatory agent. *Life Sci*. 2018;196:28–37.
- Uchegbu IF, Vyas SP. Non-ionic surfactant based vesicles (niosomes) in drug delivery. *Int J Pharm*. 1998;172(1–2):33–70.

28. Perchyonok V, Souza J, Zhang S, Moodley D, Grobler S. Bio-active designer materials and dentures: from design to application. *Int J Med Nano Res.* 2015;2:012.
29. Bonifácio BV, da Silva PB, dos Santos Ramos MA, Negri KMS, Bauab TM, Chorilli M. Nanotechnology-based drug delivery systems and herbal medicines: a review. *Int J Nanomedicine.* 2014;9:1.
30. Nie S. Understanding and overcoming major barriers in cancer nanomedicine. *Nanomedicine.* 2010;5(4):523–8.
31. Ebrahimi AK, Barani M, Sheikhshoae I. Fabrication of a new superparamagnetic metal-organic framework with core-shell nanocomposite structures: characterization, biocompatibility, and drug release study. *Mater Sci Eng C.* 2018;92:349–55.
32. Davarpanah F, Yazdi AK, Barani M, Mirzaei M, Torkzadeh-Mahani M. Magnetic delivery of antitumor carboplatin by using PEGylated-Niosomes. *DARU J Pharm Sci.* 2018:1–8.
33. Banerjee S, Kundu A. Lipid-drug conjugates: a potential nanocarrier system for oral drug delivery applications. *DARU J Pharm Sci.* 2018;26(1):65–75.
34. Hassanzadeh P, Atyabi F, Dinarvand R, Dehpour A-R, Azhdarzadeh M, Dinarvand M. Application of nanostructured lipid carriers: the prolonged protective effects for sesamol in in vitro and in vivo models of ischemic stroke via activation of PI3K signalling pathway. *DARU J Pharm Sci.* 2017;25(1):25.
35. Chen C, Zheng H, Xu J, Shi X, Li F, Wang X. Sustained-release study on Exenatide loaded into mesoporous silica nanoparticles: in vitro characterization and in vivo evaluation. *DARU J Pharm Sci.* 2017;25(1):20.
36. Barani M, Nematollahi MH, Zabolli M, Mirzaei M, Torkzadeh-Mahani M, Pardakhty A, et al. In silico and in vitro study of magnetic niosomes for gene delivery: the effect of ergosterol and cholesterol. *Mater Sci Eng C.* 2018.
37. Rameshk M, Shariffar F, Mehrabani M, Pardakhty A, Farsinejad A, Mehrabani M. Proliferation and in vitro wound healing effects of the Microniosomes containing *Narcissus tazetta* L. bulb extract on primary human fibroblasts (HDFs). *DARU J Pharm Sci.* 2018;26(1):31–42.
38. Moghassemi S, Hadjizadeh A. Nano-niosomes as nanoscale drug delivery systems: an illustrated review. *J Control Release.* 2014;185:22–36.
39. Pathak S. Bioavailability Enhancement of Poorly Water-soluble Nano Diosgenin by Encapsulation using Chitosan/Bovine Serum Albumin Bilayers. *Asian J Pharm (AJP).* 2018;12:02.
40. Wei Z, Xin G, Wang H, Zheng H, Ji C, Gu J, et al. The diosgenin prodrug nanoparticles with pH-responsive as a drug delivery system uniquely prevents thrombosis without increased bleeding risk. *Nanomedicine.* 2018;14(3):673–84.
41. Basiri L, Rajabzadeh G, Bostan A.  $\alpha$ -Tocopherol-loaded niosome prepared by heating method and its release behavior. *Food Chem.* 2017;221:620–8.
42. Addas R, Taboada P, Hajinezhad MR, Barani M, Beyzaei H. Effect of tocopherol on the properties of Pluronic F127 microemulsions: Physico-chemical characterization and in vivo toxicity. *J Mol Liq.* 2018.
43. Washington C. Drug release from microdisperse systems: a critical review. *Int J Pharm.* 1990;58(1):1–12.
44. Yeo L, Olusanya T, Chaw C, Elkordy A. Brief effect of a small hydrophobic drug (Cinnarizine) on the physicochemical characterisation of Niosomes produced by thin-film hydration and microfluidic methods. *Pharmaceutics.* 2018;10(4):185.
45. Hans M, Lowman A. Biodegradable nanoparticles for drug delivery and targeting. *Curr Opinion Solid State Mater Sci.* 2002;6(4):319–27.
46. Yang W, Hu Q, Xu Y, Liu H, Zhong L. Antibody fragment-conjugated gemcitabine and paclitaxel-based liposome for effective therapeutic efficacy in pancreatic cancer. *Mater Sci Eng C.* 2018;89:328–35.
47. Barani M, Mirzaei M, Torkzadeh-Mahani M, Nematollahi MH. Lawsone-loaded Niosome and its antitumor activity in MCF-7 breast Cancer cell line: a Nano-herbal treatment for Cancer. *DARU J Pharm Sci.* 2018;26(1):11–7.
48. Pando D, Caddeo C, Manconi M, Fadda AM, Pazos C. Nanodesign of olein vesicles for the topical delivery of the antioxidant resveratrol. *J Pharm Pharmacol.* 2013;65(8):1158–67.
49. Suriyaprakash TNK, Parthiban S, Prabu SL, Sumathi A. Formulation and evaluation of paclitaxel niosome for its improved anti-cancer activity. *ACTA Pharm Sci.* 2011;53(3).
50. Jain R, Sukla SK, Nema N, Panday A. Drug Nano-particle: a release kinetics. *J Nanosci Nanotechnol.* 2015;6(5):1.
51. Xu Y-Q, Chen W-R, Tsosie JK, Xie X, Li P, Wan J-B, et al. Niosome encapsulation of curcumin. *J Nanomater.* 2016;2016:15.
52. Han W, Wang S, Liang R, Wang L, Chen M, Li H, et al. Non-ionic surfactant vesicles simultaneously enhance antitumor activity and reduce the toxicity of cantharidin. *Int J Nanomedicine.* 2013;8: 2187.

**Publisher's note** Springer Nature remains neutral with regard to jurisdictional claims in published maps and institutional affiliations.